

Interaction of CO, O, and S with metal nanoparticles on Au(111): A theoretical study

Ping Liu, José A. Rodriguez,* James T. Muckerman, and Jan Hrbek

Department of Chemistry, Brookhaven National Laboratory, Bldg. 555, Upton, New York 11973

(Received 4 October 2002; revised manuscript received 12 December 2002; published 29 April 2003)

Density functional theory and slab models are used to study the unusual behavior of Mo, Ni and Ru nanoparticles on a Au(111) substrate. After considering several different structures and compositions for the metal nanoparticles on the Au(111) interface, the calculations show that the metal particles energetically prefer to be embedded into the surface or form Au/metal particles/Au(111) sandwich like structures. The calculations also indicate that the observed deactivation of the Mo/Au interface to CO, O₂, and S₂ adsorption is due to the passivation of Mo as a result of the intermixing between Mo and Au. Mo atoms in the substrate can be pulled out to the surface by interacting with oxygen or sulfur adatoms, eventually forming molybdenum oxides or sulfides. This process depends on a delicate balance between the adsorbate-Mo and Mo-Au interactions, and usually requires high coverages of the adsorbate. It can lead to big changes in the morphology of nanoarrays. Ru/Au(111) and Ni/Au(111) exhibit a similar behavior to that of Mo/Au(111). Thus, the phenomena described above must be taken into consideration when preparing nanoparticles on a Au template.

DOI: 10.1103/PhysRevB.67.155416

PACS number(s): 68.43.-h; 71.15.Mb; 81.07.-b; 81.16.Be

I. INTRODUCTION

Recently, the behavior of metal nanoparticles is receiving a lot of attention.¹⁻⁴ In principle, nanoparticles can have unique mechanical, electronic, optical, magnetic, and chemical properties with respect to those of bulk and single particle species⁵ and thus have many fascinating potential uses.^{6,7} For example, these systems can be useful in the fabrication of electro-magnetic devices and sensors.⁵⁻⁷ Nanoparticles also have significant potential as higher activity and selectivity catalysts for chemical and electrochemical processes.^{3,8-10}

In the emerging field of nanotechnology, a goal is to make metal nanostructure in well-defined and controlled spatial arrays. Gold surfaces are commonly used as templates for the growth of self-assembled monolayer of organic molecules.¹¹ Since gold is a chemically inert element,^{12,13} a Au(111) substrate can be an ideal template for growing and probing the physical and chemical properties of metal oxide, sulfide and carbide nanoparticles.^{1,14,15} In the first step, metals can be deposited on the Au(111) substrate either by direct evaporation^{1,16} or by decomposition of metal-carbonyl precursors.^{14,15,17} In the second step the metal nanoclusters deposited can be studied^{14,15} or undergo additional treatment to be transformed into sulfide, oxide or carbide nanoparticles.^{1,14,15} For this type of studies, it is very important to understand at a fundamental level the interactions between the gold substrate and supported metals.

Scanning tunneling microscopy (STM)^{1,17} and high-resolution photoemission¹⁵ have been used to examine the behavior of Mo particles on Au(111). The results of STM studies show the formation of nanostructures at defects, steps, and dislocations of the Au(111) substrate upon the deposition of Mo.^{1,17} The STM images do not allow a clear identification of Mo and Au atoms, and site exchange between Mo and Au could occur near the surface.¹⁸ The Mo/Au(111) systems exhibit Mo 3d_{5/2} core level binding energies that are 0.2–0.3 eV higher than those measured for bulk Mo.¹⁵ Valence photoemission spectra also show that bimetal-

lic bonding induces electronic perturbations in Mo and Au. The Mo/Au(111) surfaces ($\Theta_{\text{Mo}} < 0.3$ ML) display an extremely low reactivity towards CO, O₂, and C₂H₄.^{14,15} Thus, while surfaces of pure Mo adsorb and dissociate O₂ and CO at room temperature,^{13,19} the nanostructures in Mo/Au(111) interact poorly with the molecules even at 100 K.^{14,15} The supported Mo nanoparticles interact well with very reactive molecules like NO₂ and S₂ (MoO_x and MoS_x formation), but only at elevated temperatures.^{14,15} The modifications in the chemical properties of Mo are among the largest observed for an element in bimetallic systems.^{7,12,15,16} There are two possible explanations for the deactivation of Mo nanoparticles on Au(111). One is a combination of ligand^{16,20,21} or size³ effects. The electronic structures of Mo on the surface are modified by the Au substrate plus the limited size of the nanoparticles and therefore deactivate Mo.¹⁵ The other possible explanation is site exchange or intermixing of Mo and Au.¹⁸ The Au substrate may strongly segregate to the surface and block the interaction of adsorbates with the Mo particles. Therefore, the nanostructures exhibit a low reactivity as Au does. The existing experimental data do not allow one to establish which of these effects is responsible for the deactivation of Mo.^{15,17}

In this paper, first principle density-functional calculations are employed to study the surface morphology of Mo/Au(111) and the adsorption of CO, S, and O. By considering several different surface structures and compositions, we explore in detail relationships between the structural and chemical properties of Mo/Au(111). It is shown that the Mo particles are energetically much more stable when penetrating into the Au instead of sitting on the surface. The embedded Mo atoms are electronically perturbed and the activity of the bimetallic system is determined by the shift of these atoms from inside to above the gold substrate. These phenomena are also observed in density functional calculation for other bimetallic systems (Ni/Au and Ru/Au), and must be taken into consideration when preparing nanoparticles on Au(111).

The paper is organized as follows. We first introduce the

method of calculation and the supercell set up used to describe the configuration of Mo particles on Au(111). We then show the energetically preferred configurations according to the calculations. Based on these, we illustrate the interesting activities of the Mo particles on/in Au(111) for CO, O, and S adsorptions. Finally, we compare the behavior of several bimetallic systems formed by deposition of metals on Au(111).

II. METHOD OF CALCULATION

In the present theoretical work, we use density functional theory to calculate the formation energies and the CO, S, and O adsorption energies on various Mo/Au(111) bimetallic surfaces. The calculations are performed using the CASTEP (Cambridge Serial Total Energy Package) suite of programs,²² which have proved to be very useful in theoretical studies dealing with metal surfaces.^{23–25} The Kohn-Sham one-electron equations are solved on a basis of plane waves with kinetic energy below 25 Ry and ultrasoft pseudopotentials are used to describe the ionic cores.²⁶ We have found that the pseudopotentials used in this work reproduce well the results of all electron calculations for systems that involve Au, Mo, and S.²⁷ The K-points used are chosen so that the sampling of the Brillouin zones (BZs) for different surface unit cells is ensured using the Monkhorst-Pack scheme.²⁸ 16 K points are considered for the BZ sampling and integration in the present calculation. We have also checked that increasing the number of K points up to 64 changes the adsorption energy by less than 0.02 eV. These effects are much smaller than the effects of changing the surface composition, which is the interest of the present study. The exchange-correlation energy and the potential are described by the revised version of the Perdew-Burke-Ernzerhof functional.²⁹

The structural parameters of each system are determined using the Broyden-Fletcher-Goldfarb-Shanno minimization technique, with an energy change per atom less than 2×10^{-5} eV, residual force less than 0.05 eV/Å, and the displacement of atoms during the geometry optimization less than 0.002 Å.

In most cases, we describe the surfaces using a four-layer slab with a 2×2 unit cell, as shown in Fig. 1. The only exception is the case shown in Fig. 1(h), for which we use a five-layer slab. Previous theoretical studies have shown that four-layer slabs can be enough to describe pure metal surfaces and adsorbate/metal interfaces.^{10,23,27} For a full Mo monolayer on Au(111), [Fig. 1(b)], we obtained essentially the same results using four, six or eight Au layers to represent the substrate. In addition, very similar results were obtained after comparing the adsorption of sulfur on four- and six-layer slabs representing Au(111),²⁷ or CO on a Mo monolayer supported on three- or five layer Au slabs. The two-dimensional periodic slabs are embedded in a three dimensional periodic supercell, with a vacuum 11-Å-thick separating the top and the bottom of the slabs along the surface direction. Eight different kinds of Mo/Au(111) surfaces have been investigated (Fig. 1). They involve configurations in which the Mo is either on top of the gold surface or embedded in the first, second or third layer. The adsorption

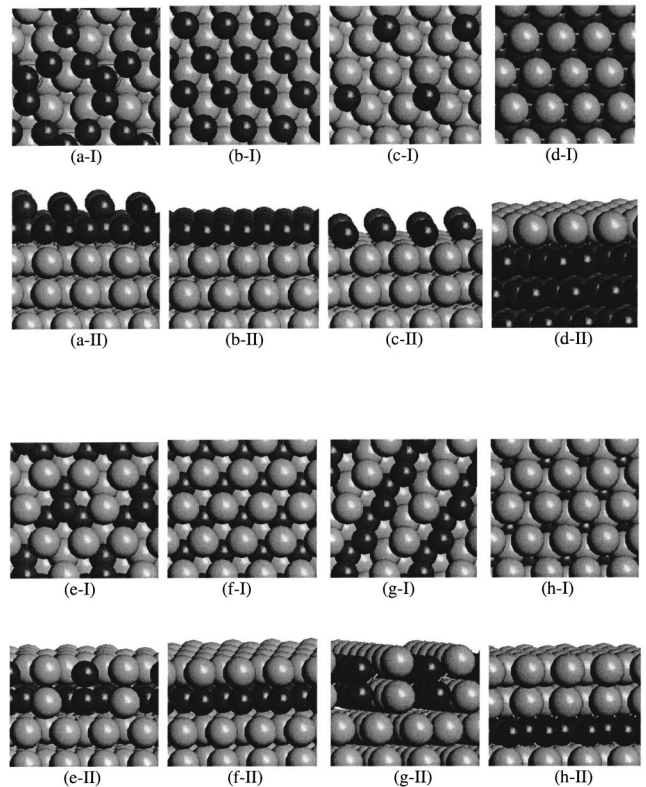


FIG. 1. Configuration of Mo/Au(111) bimetallic surfaces studied in this paper. For each configuration, “I” is the top view and “II” is the side view. The big light and dark balls represent Au and Mo, respectively.

of CO, S, and O on each Mo/Au(111) surface is also calculated. In the present study, the CO adsorption site is atop for all the cases as observed on most transition metal surfaces,³⁰ while the high coordination sites are preferred for O and S adsorption.^{21,25,31}

The calculated CO molecule, atomic O and S adsorption energy is expressed as

$$\Delta E_{\text{ads}} = E(\text{adsorbate/metal}) - E(\text{metal}) - E(\text{adsorbate}). \quad (1)$$

The dissociative adsorption energy of the molecules O_2 and S_2 is deduced from the corresponding atomic adsorption energy, which can be expressed as

$$\Delta E_{\text{ads}} = 2 * E(\text{atom/metal}) - 2 * E(\text{metal}) - E(\text{molecule}). \quad (2)$$

In all the cases under study, the adsorbates and the first three slab layers are allowed to relax in all dimensions while the metal atoms in the bottom layer are fixed at the lattice positions of the substrate.

III. CONFIGURATION OF THE Mo/Au(111) INTERFACE

To understand the interesting behavior of nanoparticles in Mo/Au(111), it is very important to know the surface composition first, which is not possible to obtain from STM experiments.¹⁷ Density functional calculations can be used to

find out the energetically favored configuration.^{18,21} The chemical composition at the surface of an alloy can differ from the composition in the bulk. If segregation occurs, one of the alloy components may enrich the surface region. A database of the surface segregation energies of single (or isolated) transition metal impurities in transition metal substrates has been presented based on quantitative first-principle calculations.^{18,21} It is shown that for single impurities, like Mo, Ni, or Ru, in Au(111), the impurities should remain in the substrate with a positive segregation energy.

In the present study, therefore, we consider the cases of Mo placed on the surface of Au, Mo intermixing with Au both in the surface and in the substrate, and Mo being totally driven into the substrate with only Au atoms in the surface. Eight different structures have been included as shown in Fig. 1, where we can see top (*I*) and side (*II*) views of each configuration. Figure 1(a) (*A-a*, in the notation below) shows the case of pyramidal Mo₄ clusters on Au(111). Figure 1(b) (*A-b*) describes the case of one Mo overlayer on Au(111). Figure 1(c) (*A-c*) stands for the case of isolated Mo atoms on the Au(111) surface in a 2×2 array. Figures 1(e)–1(h) correspond to the cases of intermixing. Figure 1(e) (*A-e*) comes from embedding Mo₄ clusters into the Au(111) substrate, whereas Figs. 1(f) (*A-f*), 1(g) (*A-g*) and 1(h) (*A-h*) result from completely or partially embedding a full layer of Mo. And finally, Fig. 1(d) (*A-d*) represents the case of a Au overlayer on Mo(110).

To describe the surface stability, we use the formation energy E_f . Here, we note that the formation energy shown in this paper is relative to bulk Mo and Au. That is, E_f of bulk Mo and Au are assumed to be zero. E_f then can be written as

$$E_f = E(\text{Mo}_x\text{Au}_{1-x}) - xE(\text{Mo}) - (1-x)E(\text{Au}), \quad (3)$$

where E is the total energy of the corresponding composition in bulk. Our DF calculations show quite clearly that the Mo atoms are more stable when penetrating into the substrate rather than sitting on the surface independently of their presence as flat overlayers or isolated clusters. As shown in Fig. 2, with a 1-ML Mo coverage, the most stable configuration is *A-f*. Mo atoms are located in the second layer with Au atoms in the surface, as shown in Fig. 1(f). In fact, we also find that driving the Mo layer further down to the third layer with two Au layers on top is a little more stable by 0.02 eV/atom. It is also shown that the more Mo atoms sit in the surface, the less stable the corresponding surface configuration. Compared with the most stable configuration (*A-f*), it becomes circa 0.01 eV/atom less stable by pulling $\frac{1}{4}$ -ML Mo to the surface (*A-e*), circa 0.04 eV/atom less stable by pulling $\frac{1}{2}$ ML (*A-g*) to the surface, and 0.25 eV/atom less stable by forming a Mo overlayer on Au(111) (*A-b*). The *A-e* configuration with Mo atoms embedded in both the surface and subsurface layers [Fig. 1(e)] is very close in energy to the *A-f* and *A-h* configurations. Thus, entropic and kinetic factors could determine the degree of penetration of Mo into the Au substrate. According to the results in Fig. 2, the formation of Mo clusters on Au(111) should not prevent the penetration of the admetal into the gold substrate. The *A-a* configuration is circa 0.3 eV/atom less stable than the *A-e* configuration.

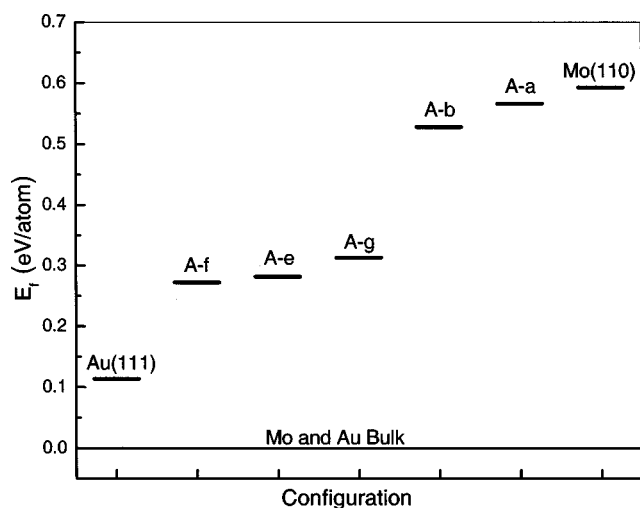


FIG. 2. Formation energy of Au(111), Mo(110) and Mo/Au(111) systems. Here, the formation energy is relative to bulk Mo and Au. That is, we assume here that the formation energies of both bulk Mo and Au are equal to zero. The coverage of Mo for the different Mo/Au(111) systems is 1 ML. “A” represents the Mo/Au alloy. “a”–“g” labels correspond to the configurations shown in Fig. 1.

Therefore, even Mo clusters energetically prefer to be driven into the substrate instead of staying on the surface. The behavior seen for the Mo aggregates on Au(111) is consistent with Green function linear muffin-tin orbitals calculations for Mo impurities in Au(111), where the energy cost to remove Au from the surface is 0.67 eV/atom.^{18,21} A comparison of the surface free energies of pure Au(0.10 eV Å⁻²) (Ref. 32) and Mo(0.18 eV Å⁻²) (Ref. 32) also suggests that gold should be the dominant element in the surface of Mo/Au alloys

In the present study, we only consider the case of Mo deposited on the ideal flat Au surface. In many situations, the real Au(111) surface undergoes a herringbone reconstruction.^{33,34} STM images show that the Mo atoms easily aggregate and form nanostructures on the elbows of the herringbone structure.^{1,17} The Au atoms in such elbows are under stress and more reactive towards Mo than atoms in an ideal flat terrace of Au(111).^{1,35,36} The Mo atoms deposited on the elbows then act as preferential nucleation centers for trapping additional Mo atoms and forming clusters.^{37,38} According to our calculations, the binding energy of a free Mo atom on a Au(111) surface with already $\frac{1}{4}$ ML Mo is almost two times bigger than that on pure Au(111). The reason is that the admetal-admetal bonding is stronger than the admetal-Au bonding. Thus a free diffusing Mo atom would be eventually trapped by the Mo adsorbed on the elbows. Therefore, STM observes the formation of nanostructures on the elbows of the herringbone structure.^{1,17} The same is valid for Fe,³⁹ Co,⁴⁰ Ni,^{41,42} Pd,⁴³ Rh,⁴⁴ and Ru (Ref. 45) deposition on Au(111). On the contrary, preferential nucleation is not observed if the admetal-admetal bonding is not strong enough compared with admetal-Au bonding, such as the cases of Al,⁴⁶ Cu,⁴⁷ Ag,⁴⁸ and Au (Ref. 49) deposition on Au(111).

TABLE I. Calculated adsorption energies (eV). “A” represents a MoAu alloy. “a” to “g” is corresponding to the configuration shown in Fig. 1.

	$E_{\text{ads}}^{\text{CO}}$ (eV/molecule)	$E_{\text{ads}}^{\text{O}}$ (eV/atom)	$E_{\text{ads}}^{\text{O}_2}$ (eV/molecule)	$E_{\text{ads}}^{\text{S}}$ (eV/atom)	$E_{\text{ads}}^{\text{S}_2}$ (eV/molecule)
Mo(110)	-1.89	-6.81	-8.36	-6.08	-6.97
Au(111)	0.07	-2.02	1.22	-3.23	-1.28
A-a	-2.22	-7.51	-9.76	-6.30	-7.41
A-b	-2.79	-7.69	-10.14	-7.00	-8.81
A-c	-1.91	-6.69	-8.12	-5.76	-6.33
A-d	-0.11	-2.41	0.44	-3.50	-1.81
A-e	-1.03	-4.75	-4.24	-4.16	-3.14
A-f	-0.35	-2.05	1.16	-3.39	-1.59
A-g	-0.93	-5.18	-5.11	-4.58	-3.98

As we mentioned above, the Mo atoms form particles at the elbows of the herringbone of Au(111). On the other hand, we also indicate that the Mo atoms prefer to be driven into the gold substrate. The combination of these two phenomena leads to a complex situation. This raises an important question. Are the Mo atoms deposited on the elbows above the surface or in the substrate during the growth of the nanoparticles? We suggest that the Mo atoms are located on or near the surface during the dosing and forming of the nanoparticles. Once the formation of a Mo particle is completed, the Au atoms would begin to site exchange with Mo or segregate to the surface. This could generate a sandwich structure with Mo atoms occupying sites in the substrate and Au atoms on top. As we will see below, the idea of Mo-Au site exchange and Au segregation is consistent with the chemical behavior found for the Mo/Au(111) surfaces. The chemical activities of these bimetallic systems seem to be determined by the shifts of Mo atoms from inside to above the gold surface.

IV. SURFACE REACTIVITY

In the present paper, we use CO, O, and S adsorption as the probes to study the chemical activities of all the Mo/Au alloy surfaces. By comparing our results for adsorption on well-defined sites of the surface to experimental data,^{14,15} we obtain a direct indication of the morphology of the Mo/Au(111) systems.

A. CO adsorption

The interaction of CO with bimetallic systems has been the subject of many works.^{12,16,20,21,50} The strength of the CO adsorption bond is very sensitive to electronic perturbations induced by bimetallic bonding.^{20,21,50} The distribution of electrons around the metal centers and shifts in the valence d bands can have a strong influence in the CO adsorption energies.^{12,20} Results of core-level photoemission show no big electronic perturbations after depositing Mo on Au(111).¹⁵ But the changes in the CO chemisorption properties of Mo are very large, and Mo/Au(111) surfaces are unable to adsorb CO at 300 K under ultrahigh vacuum conditions.¹⁵ This unusual behavior can be attributed to a consequence of combining the limited size of the Mo nano-

particles with the effects of Mo-Au interactions, without including Mo-Au intermixing.¹⁵ The validity of this hypothesis can be tested using density functional (DF) calculations.²¹

It has been reported that CO strongly bonds and easily dissociates on Mo(110),¹⁹ while has no interaction with Au(111).⁵¹ The DF results in Table I show that CO bonds well to a Mo(110) surface ($\Delta E_{\text{ads}} = -1.89$ eV), while a Au(111) surface interacts weakly with CO ($\Delta E_{\text{ads}} = 0.07$ eV), in agreement with previous theoretical studies.^{29,52} We have considered CO adsorption on the various Mo/Au bimetallic surfaces displayed in Fig. 1. It can be seen in Table I that the adsorption energies change a lot with different surface compositions and configurations.

For the case of 1 ML of Mo₄ clusters (*A-a*) and a pseudomorphic Mo overlayer sitting on the surface of Au (*A-b*) as shown in Figs. 1(a) and 1(b), the Mo-CO bonding strengths are even much stronger than that for the case of Mo(110). The activation of Mo is due to electronic modification caused by ligand or size effects. In these configurations, the Mo-Mo bonds are stretched with respect to Mo(110) and thus the d band of Mo becomes narrow with its center (ϵ_d) shifting up (circa 1 eV) towards the Fermi level to keep the d filling. It has been found that the bonding of an adsorbate with a metal surface becomes stronger with ϵ_d shifting up, and vice versa.^{21,53–55} Therefore, Mo-CO bonding in *A-a* and *A-b* then becomes stronger (Table I). In addition, after decreasing the Mo particle size from pyramidal Mo₄ clusters (*A-a*) to isolated Mo atoms (*A-c*), the Mo-CO bond is still very strong by reducing its strength only 0.3 eV. From these results, we can conclude that any Mo atom or cluster located above Au(111) should bond CO strongly, a trend not consistent with the experimental observations.¹⁵

With $\frac{1}{2}$ ML of Mo driven into the substrate (*A-g*), the CO adsorption energy decreases ($\Delta E_{\text{ads}} = -0.93$ eV), which we speculate to be partly due to the decreasing number of Mo neighbors in the surfaces (ligand effect) and to steric blocking of the Mo-CO interaction by gold. The same phenomena occur when further driving $\frac{3}{4}$ ML of Mo atoms into the substrate (*A-e*), and the CO adsorption energy becomes -1.03 eV, which is also considerably weaker than for pure Mo. Finally, we reach the case *A-f*. With only Au atoms in the surface and the Mo atoms in the substrate, CO cannot inter-

TABLE II. Calculated surface stabilities before and after the adsorption of CO, O, or S. ‘‘A-a~A-g’’ represent the Mo/Au(111) alloy surfaces with different configurations, which are the same as shown in Fig. 2 and Table I. The energies for all the cases shown here are relative to the case of A-f and correspond to the energy of the four-layer 2×2 supercells with one layer of Mo atoms and three layers of Au atoms. The coverage of all the adsorbates is $\frac{1}{4}$ ML. The exceptions are the values in parentheses, which correspond to a full monolayer of sulfur on the surface.

	Clean surface (eV)	CO/surface (eV/molecule)	O/surface (eV/atom)	S/surface (eV/atom)
A-f	0	0	0	0
A-a	4.70	2.82	-0.07	1.74
A-b	4.07	1.64	-1.57	0.41 (-3.36)
A-e	0.45	-0.53	-2.55	-0.67
A-g	0.65	0.06	-2.48	-0.59

act with Mo and the adsorption energy drops to -0.35 eV. It appears that the configurations in which a skin of Au covers Mo have an almost negligible reactivity towards CO.

In order to explain the chemical deactivation of Mo/Au(111) observed experimentally,^{14,15} it seems that one has to involve Mo-Au site exchange or Au segregation. Before we reach this conclusion, there is another issue we should consider. It has been found that adsorption can significantly change the surface composition of bimetallic alloys.^{16,55,56} We wonder whether it is possible for CO to pull the Mo back to the surface of Mo/Au alloys to form a much stronger Mo-CO bond. Thermodynamically, it would be very difficult for a few CO molecules ($\frac{1}{4}$ ML) to move the Mo atoms from the inside to above the Au substrate (see Table II). But the situation changes at higher coverage of CO. As shown in Fig. 3(a), we begin with a Mo/Au(111) bimetallic surface with Mo in the substrate which is the most stable in energy without CO present. After exposure to $\frac{3}{4}$ ML of CO, the configuration shown in Fig. 3a is not stable at all. The calculations

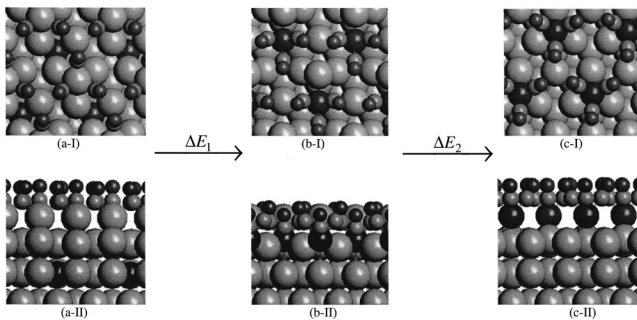


FIG. 3. Configuration change before (a) and after (b), (c) depositing $\frac{3}{4}$ ML of CO on a Mo/Au(111) surface ($\Theta_{\text{Mo}} = \frac{1}{4}$ ML). For each configuration, ‘‘I’’ is the top view and ‘‘II’’ is the side view. The big light and dark balls represent Au and Mo, respectively. The small light and dark balls represent carbon and oxygen, respectively. (a) The reactant $\frac{3}{4}$ ML of CO deposited on Mo/Au(111) with Mo inside the substrate. (b) The intermediate CO molecules pulling Mo from the substrate to the surface edge. (c) Product, CO molecules pulling Mo to above the surface of Au.

indicate that a Fig. 3(a) \Rightarrow Fig. 3(b) transformation is a highly exothermic reaction ($\Delta E_1 = -2.99$ eV) with Mo being pulled out to the edge (half-embedded) by three CO molecules. In addition, the CO molecules pulling Mo from the edge [Fig. 3(b)] to the surface of Au [Fig. 3(c)] is also an exothermic transformation with a reaction energy, ΔE_2 , of -0.43 eV. It is therefore clearly seen that, at high CO coverage, Mo in the substrate becomes energetically unstable and should move to the surface to allow CO strongly adsorb. Under the ultrahigh vacuum conditions of the experiments in Ref. 15, the coverage of CO is very low on the surface and the Mo/Au(111) interfaces eventually behave as Au(111). To see a CO induced migration of embedded Mo to the surface, substantial pressures of CO are necessary. Recent STM experiments show results which are consistent with this idea.^{21,57}

In summary, according to this theoretical study, Mo-Au site exchange and Au segregation are the reasons for the low reactivity towards CO of the nanostructures in Mo/Au(111). The idea that the Mo nanoparticles have special chemical properties due to their limited size^{4,7,11,15} and/or Mo-Au electronic interactions¹⁵ can be ruled out.

B. Oxygen adsorption

Molybdenum oxides are widely used for the transformation of hydrocarbons in the chemical industry⁵⁸ and a general interest exists for preparing arrays of well-defined MoO_x nanoparticles. Therefore, it is worthwhile to examine the adsorption of oxygen on the nanostructures in Mo/Au(111) systems.^{14,17} Figure 4 shows a summary of experimental results for the formation of MoO_x on Au(111).^{14,17} The dosing of O_2 to Mo/Au(111) ($\Theta_{\text{Mo}} = 0.05$ ML) at 300–850 K produces no changes in the Mo 3d core levels [Fig. 4(a)]. The nanostructures in Mo/Au(111) are unreactive towards O_2 ,^{14,17} although the surface of pure Mo readily adsorbs and dissociate the oxygen molecule.¹³ In addition, the experiments also show that MoO_x nanoparticles are formed when reacting Mo/Au(111) with a strong oxidant like NO_2 [Fig. 4(b)]. Surprisingly, this oxidation process is accompanied by a very large increase in the Mo 3d intensity measured in photoemission [Fig. 4(c)]. Such a phenomenon is very hard to explain, because the adsorption of oxygen on the surface should attenuate the Mo 3d signals if Mo nanoparticles are spreaded-out above the Au substrate.

Before turning to the Mo/Au systems, we first study the adsorption on pure surfaces. It is well known that O strongly bonds with Mo.^{59–61} As shown in Table I, our calculation also indicates that Mo-O bonding is very strong with atomic adsorption energy of -6.81 eV. The O_2 adsorption energy is -8.36 eV. For O_2 adsorption on Au(111), the calculated adsorption energy is 1.22 eV. It indicates that O_2 does not adsorb at all on Au(111) as observed in the experiment,¹⁴ although the O-Au bonding for atomic O is not negligible with an adsorption energy of -2.02 eV.

Similar to the case of CO adsorption, it is shown in Table I that the O adsorption energies are much bigger for the surface alloys with Mo atoms in the surface compared to those with Mo atoms in the substrate. The O adsorptions on

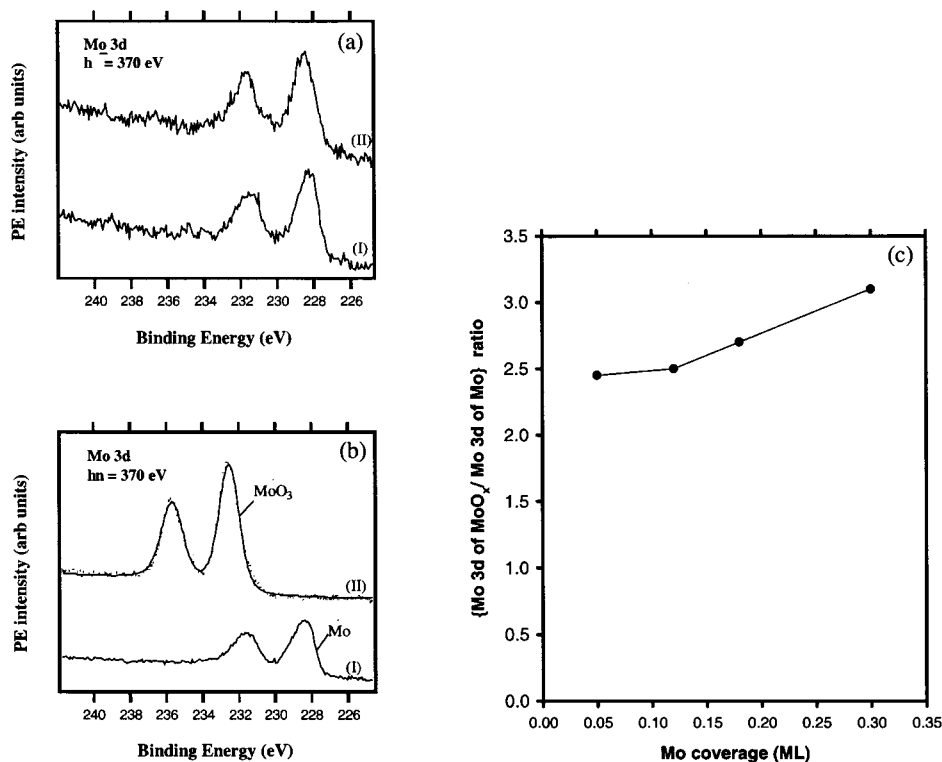


FIG. 4. (a) Mo 3d core level spectra taken before (I) and after (II) dosing 150 L of O₂ to 0.05 ML of Mo on Au(111) at 850 K. (b) Mo 3d core level spectra taken before (I) and after (II) dosing 0.5 langmuir of NO₂ to 0.05 ML of Mo on Au(111) at 500 K. (c) Ratio of the Mo 3d signals before and after oxidation of Mo in Mo/Au(111) as a function of Mo coverage. (From Ref. 14.)

both *A-a* and *A-b* are even stronger than the case of O/Mo(110) by almost 1 eV, which is due to ligand and size effects as indicated in Sec. IV A. Thus, the *A-a* and *A-b* configurations exhibit an affinity for oxygen which is not seen in the experimental measurements for O₂/Mo/Au(111).^{14,17} With the decreasing surface composition of Mo to $\frac{1}{2}$ ML (*A-g*) and $\frac{1}{4}$ ML (*A-e*), the O adsorption energy drops to -5.18 and -4.75 eV, respectively. The weakening of O bonding is mostly ascribed to the decreasing numbers of high-fold Mo sites on the surface (ensemble effect) as compared with the case *A-a* and *A-b*. For the case *A-f*, the O bonding strength drops further down close to that of O/Au(111). The corresponding adsorption energy is -2.05 eV, while the O₂ adsorption energy for the case *A-f* is only 1.16 eV, which also indicates that O₂ does not adsorb although the O adsorption energy is substantial (-2.05 eV). Similarly as seen for the CO adsorption, the O adsorption is very strong when Mo is sitting on the Au substrate (*A-a,b*), and becomes much weaker than O/Mo(110) for the case of Mo intermixing with Au (*A-e,g*) and Mo completely embedded in the substrate (*A-f*). Considering the deactivation of Mo/Au(111) to O₂ adsorption observed in photoemission experiments,¹⁸ it seems again that Mo particles should be intermixing with Au or embedded in the substrate.

Mo energetically prefers to stay on the surface in the presence of O (Table II). Configurations with Mo being pulled out to form Mo-O bonds are up to 2.55 eV (*A-e*) more stable than those with Mo in the substrate (*A-f*). However, O adatoms cannot form by O₂ exposure to the Mo/Au(111) alloy surfaces, since O₂ does not interact well with Au-rich surfaces (Table I). Therefore, no reaction is observed in the experiment when exposing to O₂.¹⁴ As for the strong oxidation ability of NO₂, we consider that it is simply because the

dissociation barrier of nitrogen dioxide (NO₂ → NO_{gas} + O_{ads}) is lower by about 1.58 eV than that for O₂ according to our calculations. Therefore, O atoms would be more easily formed by NO₂ dissociation on a Mo/Au(111) surface than O₂. Once the O adatoms are generated from NO₂, they can pull the Mo in the substrate out to the surface and form Mo oxides due to the strong interaction between O and Mo. This processes of Mo migration easily explains the gain in Mo 3d intensity seen during the oxidation of Mo/Au(111) (Fig. 4). Initially, many of the Mo atoms in the Au substrate are not detectable at the photon energy used in the experiments due to the limited escape-depth of the photo electrons.¹³ Upon migration to the surface, they become “visible” and the Mo 3d signal increases.

C. Sulfur adsorption

In technological applications molybdenum sulfide is extensively employed as a lubricant and as a catalyst for the removal of the sulfur from the petroleum.⁶² Environmental regulations stress the need for cleaner oil-derived products and there is a continuous search for better desulfurization catalysts.⁶² Well-defined arrays of MoS_x nanoparticles offer interesting possibilities in this respect.^{1,15} Figure 5 summarizes experimental results for the reaction of sulfur with Mo/Au(111) surfaces.¹⁵ In a series of experiments a Mo/Au(111) ($\Theta_{\text{Mo}}=0.05$ ML) surface was fully covered by a layer of sulfur at 300 K and heated to higher temperatures [Fig. 5(a)]. Although the system is very rich in sulfur and MoS_x is the most stable species in S/Mo/Au(111), the formation of the sulfide is not observed until heating to elevated temperatures (>600 K).¹⁵ A similar result was found at higher coverage of Mo.¹⁵ Furthermore, the formation of MoS_x is accompanied

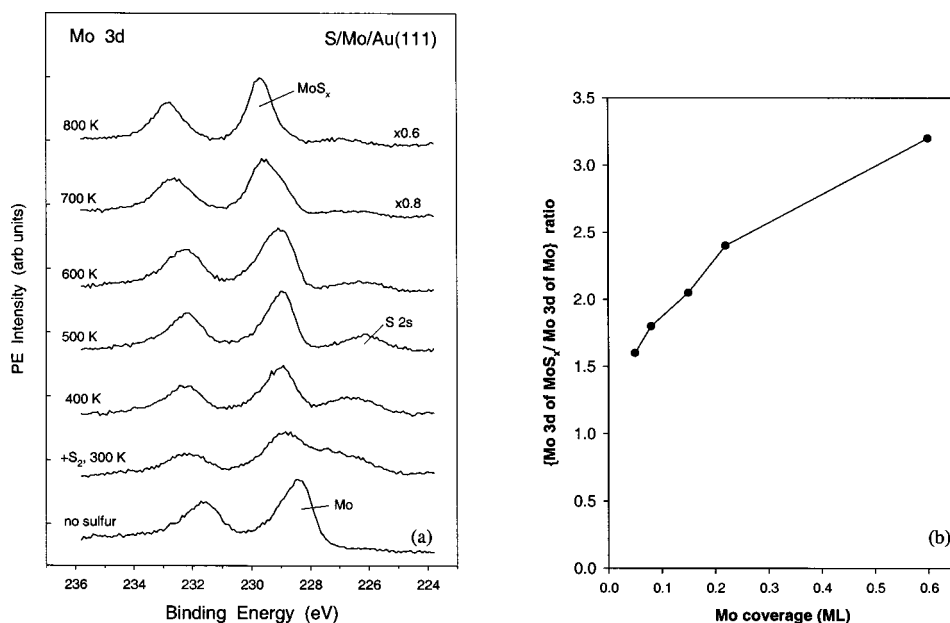


FIG. 5. (a) Mo 3d core level spectra for the adsorption of sulfur on 0.05 ML of Mo on Au(111). The surface was saturated with a layer of sulfur at 300 K and the system was heated to the indicated temperatures. (b) Ratio of the Mo 3d intensity before and after sulfidation of Mo in Mo/Au(111) as a function of Mo coverage. (From Refs. 15 and 62).

by an increase in the Mo 3d signal in photoemission [Fig. 5(b)],¹⁵ a trend which is very difficult to explain if sulfur is converting Mo nanoparticles spread out above Au(111). These phenomena need an explanation.

As reported for sulfur adsorption on Mo(110),^{63,64} our calculations also indicate that sulfur and pure Mo surfaces have a strong interaction as shown in Table I. The calculated S and S₂ adsorption energies on Mo(110) are -6.08 and -6.97 eV, respectively. The DF calculation gives a substantial adsorption energy for S on Au(111), which is also found in recent theoretical studies.^{27,31} It also predicts that S₂ does adsorb on Au(111) but the bonding is not very strong with an adsorption energy of -1.28 eV. For a total sulfur coverage of 0.25 ML, the S₂ molecule dissociates spontaneously into S atoms on Mo(110) and Au(111).^{27,65}

According to our calculations Mo atoms of clusters sitting on Au(111) should not have any problem reacting with sulfur atoms. In fact, the Mo-S bonds for the cases A-a,b are even stronger than that of S/Mo(110). By gradually driving the Mo atoms into the substrate, the surface-S bond becomes weaker as shown for the cases A-e,g and gets close to that of S/Au(111) for the case A-f, in which all the Mo atoms are inside the substrate with only Au atoms in the surface. As indicated for CO and O adsorption, the observed deactivation of Mo/Au(111) (Ref. 15) is due to Mo-Au site exchange and the presence of a gold skin over the Mo nanoparticles.

Similar as for CO and O, the configurations with Mo in the surface are also stabilized by the presence of S (Table II). Considering the case of forming MoS₂, the DF results show that the configurations with Mo being pulled out by S (A-e) are more stable than A-f. Since S₂ interacts well with Au-rich surfaces (A-f), there is no problem for the formation of atomic S by dissociating S₂.⁶⁵ However, compared with the case of oxidation, the enthalpy contribution from S-Au bonding to S-Mo bonding (Table II) seems not strong enough to overcome the kinetic barrier for Mo shifting at low sulfur coverages. To make molybdenum sulfide, one possibility is to increase the mobility of the embedded Mo atoms by rais-

ing the temperature. As observed in the experiment,¹⁵ molybdenum sulfide cannot form on Mo/Au(111) at low temperature. By raising the temperature to 800 K, the formation of MoS_x is observed in the experiment.¹⁵ Therefore, the major trend in the photoemission results of Fig. 5 (high temperature formation of MoS_x with a simultaneous large increase in the Mo 3d signal) can be explained by the migration of Mo from the bulk to the surface of the system. We take one reaction as an example for the case of high S coverage. A full ML of sulfur is deposited on a Mo/Au(111) surface with the most stable configuration A-f [Fig. 6(a)]. Under these conditions, the DF results indicate that one must have adsorbed S₂ molecules instead of S atoms, in agreement with results of core-level photoemission for this systems.¹⁵ At large surface cov-

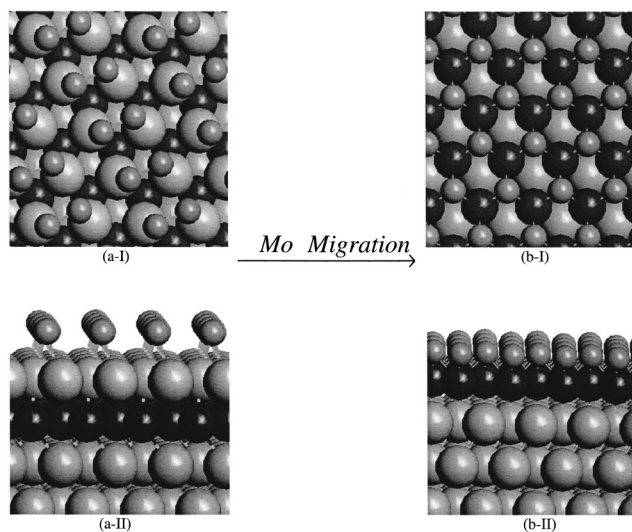


FIG. 6. Configuration change before (a) and after (b) depositing 1 ML of sulfur on Mo/Au(111) ($\Theta_{\text{Mo}} = 1$ ML). For each configuration, "I" is the top view and "II" is the side view. The big light and dark balls represent Au and Mo, and the small balls represent sulfur, respectively.

TABLE III. Calculated surface stabilities and adsorption energy of oxygen (eV/atom). “ $A-b'$,” “ $A-e'$ ” and “ $A-f'$ ” in the table indicate that the Ru(Ni)/Au(111) surface alloys have the same configurations as shown in Figs. 1(b), (e) and (f) substituting Ru (Ni) for Mo. The energies of the clean surface and O/surface shown in the table are relative to the case of $A-f'$ and correspond to the energy of the four-layer 2×2 supercells with one layer of Mo atoms and three layers of Au atoms. The coverage of oxygen for all the cases is $\frac{1}{4}$ ML.

	Ru/Au(111)			Ni/Au(111)		
	$A-b'$	$A-e'$	$A-f'$	$A-b'$	$A-e'$	$A-f'$
Surface	2.02	-0.48	0	2.48	0.46	0
O/surface	-1.75	-2.52	0	-1.12	-0.94	0
$E_{\text{ads}}^{\text{O}}$	-5.84	-4.12	-2.08	-5.63	-3.44	-2.04
$E_{\text{ads}}^{\text{O}_2}$	-6.43	-2.98	1.10	-6.01	-1.62	1.18

erages, gold surfaces bond the adsorbate but are not able to dissociate the S_2 molecule.^{15,27} The calculation shows that a complete migration of Mo from the second layer to the surface by the dissociated S atoms [Fig. 6(b)] is highly exothermic ($\Delta E = -3.36$ eV).

V. BEHAVIOR OF Ru/Au(111) AND Ni/Au(111) SURFACE ALLOYS

Au(111) is frequently used as a template for growing and probing the physical and chemical properties of metal nanoparticles.^{1,15,40-46} Many admetals can intermix or site-exchange with gold.¹⁸ It is worthwhile to examine how general are the phenomena seen above for Mo/Au(111). Both Ru/Au(111) and Ni/Au(111) surface alloys are also studied in this paper. As we will see, these two systems exhibit a similar behavior to Mo/Au(111) alloys.

Here we consider each bimetallic system with three kinds of configurations, $A-b'$, $A-e'$ and $A-f'$. They have exactly the same atomic arrangement for Mo/Au(111) shown in Figs. 1(b), 1(e), and 1(f), respectively, by substituting Ru or Ni for Mo. The DF results are shown in Table III. These indicate that, like Mo, Ni also prefers to be embedded in the substrate rather than on the surface, which is also shown by a previous theoretical and experimental study.⁶⁶ The configurations become less stable by 0.46 and 2.48 eV with pulling $\frac{1}{4}$ ML ($A-e'$) and 1 ML ($A-b'$) Ni from the substrate ($A-f'$) to the surface, respectively. Similarly for Ru/Au(111) systems, the configuration of 1-ML Ru sitting on Au(111) ($A-b'$) is 2.02 eV less stable than $A-f'$ with all Ru occupying the second layer, while, by pulling of a $\frac{1}{4}$ of 1 ML of Ru to the surface $A-e'$ is a little bit more stable.

Oxygen adsorption on Ru/Au(111) and Ni/Au(111) is also included in Table III. Similarly to the case of Mo/Au(111), our calculations show (Table III) that Ru/Au(111) and Ni/Au(111) are deactivated and behave like Au when Ru or Ni migrate into the substrate and Au is on the surface. In addition, it is also found that the Ru or Ni atoms on the surface can be stabilized in presence of O atoms. Compared with the configuration $A-f'$, the configurations with Ru or Ni on the surface, $A-b'$ and $A-e'$, become 1 or 2 eV more stable after adsorbing $1/4$ of a monolayer of atomic oxygen. Thus, Ru or Ni atoms in the substrate can be pulled out to the surface by

atomic O. There is a delicate balance between the oxygen-admetal and admetal-gold interaction, and the presence of oxygen can completely modify the morphology of a nanoarray in Ru/Au(111) and Ni/Au(111).

VI. SUMMARY

DFT periodic slab calculations were used to study the configuration and chemical activity of metal (Mo, Ni, Ru) nanoparticles on Au(111) interfaces. The results show that there is a strong site exchange or intermixing between the metal nanoparticles in the surface and the Au in the substrate. The most energetically favorable structure is a sandwich structure with the atoms of the nanoparticles driven into the substrate and Au atoms segregating to the surface. But kinetic or entropic effects could limit the penetration of the metal nanoparticles into the Au substrate.

The calculations show that the reason for the experimentally observed deactivation of metal nanoparticles is due to site exchange and not ligand or size effects. Mo atoms on top of Au(111) bond CO, O₂, and S₂ more strongly than the atoms in Mo(110) due to an upward shift of the d valence band of the metal atoms in the nanoparticles. Once metal nanoparticles are embedded inside gold, interactions with molecules such as CO, O₂ and S₂ are difficult and the bimetallic interface behaves mostly like gold under ultra high vacuum conditions.

The calculations also indicate that large coverages of an adsorbate (CO, O, and S for example) will pull the metal nanoparticles back to the surface. For O₂ and S₂ adsorption, a critical factor is the formation of O and S atoms or the dissociation barrier of the molecule. NO₂ with a lower dissociation barrier than O₂ offers a convenient route to produce large coverage of atomic oxygen. Also substantial pressures of CO or O₂ can produce adsorbate coverage that eventually will lead to a change in the morphology of the interfaces. In fact, such behavior is similar to that of metal nanoparticles on oxide surfaces as reported in a recent experiment,⁶⁷ where the shape of the nanoparticles changes under a gas environment. Thus, the phenomena described above must be taken into consideration when preparing nanoparticles on some specific template.

ACKNOWLEDGMENTS

The authors would like to acknowledge thought-provoking conversations with Z. Song, T. Cai, A. S. Y. Chan and C. M. Friend. This research was carried out at Brookhaven National Laboratory under contract DE-AC02-

98CH10886 with the US Department of Energy, Division of Chemical Sciences. The spectra shown in Figs. 4 and 5 were acquired at the national Synchrotron Light Source (NSLS), which is supported by the Material and Chemical Sciences Divisions of the U.S. Department of Energy.

- *Corresponding author. FAX: +1-631-344-5815. Email address: rodriguez@bnl.gov
- ¹S. Helveg, J. V. Lauritsen, E. Lægsgaard, I. Stensgaard, J. K. Nørskov, B. S. Clausen, H. Tøpsoe, and F. Besenbacher, *Phys. Rev. Lett.* **84**, 951 (2000).
 - ²L. Giordano, J. Goniakowski, and G. Pacchioni, *Phys. Rev. B* **64**, 075417 (2001).
 - ³J. A. Rodriguez, G. Liu, T. Jirsak, J. Hrbek, Z. P. Chang, J. Dvorak, and A. Maiti, *J. Am. Chem. Soc.* **124**, 5242 (2002).
 - ⁴Z. Yang, R. Wu, and D. W. Goodman, *Phys. Rev. B* **61**, 14066 (2000).
 - ⁵E. Cattaruzza, G. Battaglin, F. Gonella, R. Polloni, G. Mattei, C. Maurizio, P. Mazzoldi, C. Sada, M. Montagna, C. Tosello, and M. Ferrari, *Philos. Mag. B* **82**, 735 (2002).
 - ⁶U. Simon, G. Schon, and G. Schmid, *Angew. Chem., Int. Ed. Engl.* **36**, 910 (1997).
 - ⁷R. Elghanian, J. J. Storhoff, R. C. Mucic, R. L. Letsinger, and C. A. Mirkin, *Science (Washington, DC, U.S.)* **277**, 1078 (1997).
 - ⁸S. Ozkar and R. G. Finke, *J. Am. Chem. Soc.* **124**, 5796 (2002).
 - ⁹J. A. Widegren, J. D. Aiken, S. Ozkar, and R. G. Finke, *Chem. Mater.* **13**, 312 (2001).
 - ¹⁰F. Besenbacher, I. Chorkendorff, B. S. Clausen, B. Hammer, A. M. Molenbroek, J. K. Nørskov, and I. Stensgaard, *Science* **279**, 1913 (1998).
 - ¹¹Y. Yourdshahyan, H. K. Zhang, and A. M. Rappe, *Phys. Rev. B* **63**, 081405 (2001).
 - ¹²B. Hammer, Y. Morikawa, and J. K. Nørskov, *Phys. Rev. Lett.* **76**, 2141 (1996).
 - ¹³K. Hayek and H. E. Farnsworth, *Surf. Sci.* **10**, 429 (1968).
 - ¹⁴Z. P. Chang, Z. Song, G. Liu, J. A. Rodriguez, and J. Hrbek, *Surf. Sci. Lett.* **512**, L353 (2002).
 - ¹⁵J. A. Rodriguez, J. Dvorak, T. Jirsak, and J. Hrbek, *Surf. Sci.* **490**, 315 (2001).
 - ¹⁶J. A. Rodriguez, *Surf. Sci. Rep.* **24**, 232 (1996).
 - ¹⁷Z. Song, T. Cai, J. A. Rodriguez, J. Hrbek, A. S. Y. Chan, and C. M. Friend, *J. Phys. Chem. B* **107**, 1036 (2003).
 - ¹⁸A. V. Ruban, H. L. Skriver, J. K. Nørskov, *Phys. Rev. B* **59**, 15 990 (1999).
 - ¹⁹A. J. Jaworowski, M. Smedh, M. Borg, A. Sandell, A. Beulter, S. L. Sorensen, E. Lundgren, and J. N. Andersen, *Surf. Sci.* **492**, 185 (2001).
 - ²⁰R. Wu and A. J. Freeman, *Phys. Rev. B* **52**, 12 419 (1995).
 - ²¹B. Hammer and J. K. Nørskov, *Adv. Catal.* **45**, 71 (2000).
 - ²²M. C. Payne, D. C. Allan, T. A. Arias, and J. D. Johannopoulos, *Rev. Mod. Phys.* **64**, 1045 (1992).
 - ²³J. A. Rodriguez, J. M. Ricart, A. Clotet, and F. Illas, *J. Chem. Phys.* **115**, 454 (2001).
 - ²⁴Z. Yang, R. Wu, and J. A. Rodriguez, *Phys. Rev. B* **65**, 155409 (2002).
 - ²⁵M. Chen, P. G. Clark, Jr., T. Mueller, C. M. Friend, and E. Kaxiras, *Phys. Rev. B* **60**, 11 783 (1999).
 - ²⁶D. Vanderbilt, *Phys. Rev. B* **41**, 7892 (1990).
 - ²⁷J. A. Rodriguez, J. Dvorak, T. Jirsak, G. Liu, J. Hrbek, Y. Aray, and C. Gonzalez, *J. Am. Chem. Soc.* **125**, 276 (2003).
 - ²⁸H. J. Monkhorst and J. D. Pack, *Phys. Rev. B* **12**, 5188 (1976).
 - ²⁹B. Hammer, L. B. Hansen, and J. K. Nørskov, *Phys. Rev. B* **59**, 7413 (1999).
 - ³⁰P. J. Feibelman, B. Hammer, J. K. Nørskov, F. Wagner, M. Scheffler, R. Stumpf, R. Watwe, and J. Dumesic, *J. Phys. Chem. B* **105**, 4018 (2001).
 - ³¹J. Gottschalck and B. Hammer, *J. Chem. Phys.* **116**, 784 (2002).
 - ³²L. Z. Mezey and J. Gibei, *J. Appl. Phys.* **21**, 1569 (1982).
 - ³³J. Jacobsen, K. W. Jacobsen, and P. Stoltze, *Surf. Sci.* **317**, 8 (1994).
 - ³⁴K. G. Huang, D. Gibbs, D. M. Zehner, A. R. Sandy, and S. G. J. Mochrie, *Phys. Rev. Lett.* **65**, 3313 (1990).
 - ³⁵H. Dietrich, P. Geng, K. Jacobi, and G. Ertl, *J. Chem. Phys.* **104**, 375 (1996).
 - ³⁶R. Kose, W. A. Brown, and D. A. King, *J. Am. Chem. Soc.* **121**, 4845 (1999).
 - ³⁷J. A. Meyer, I. D. Baikie, E. Kopatzki, and R. J. Behm, *Surf. Sci. Lett.* **365**, L647 (1996).
 - ³⁸J. A. Meyer and R. J. Behm, *Surf. Sci.* **322**, L275 (1995).
 - ³⁹J. Wollschläger and N. M. Amer, *Surf. Sci.* **277**, 1 (1992).
 - ⁴⁰V. Repain, J. M. Berroir, S. Rousset, and J. Lecoeur, *Surf. Sci.* **447**, L152 (2000).
 - ⁴¹W. G. Cullen and P. N. First, *Surf. Sci.* **420**, 53 (1999).
 - ⁴²F. A. Moller, O. M. Magnussen, and R. J. Behm, *Phys. Rev. Lett.* **77**, 5249 (1996).
 - ⁴³A. W. Stephenson, C. J. Baddeley, M. S. Tikhov, and R. M. Lambert, *Surf. Sci.* **398**, 172 (1998).
 - ⁴⁴I. Chado, F. Scheurer, and J. P. Bucher, *Phys. Rev. B* **64**, 094410 (2001).
 - ⁴⁵S. Strbac, F. Maroun, O. M. Magnussen, and R. J. Behm, *J. Electroanal. Chem.* **500**, 479 (2001).
 - ⁴⁶B. Fischer, J. V. Barth, A. Fricke, L. Nedelmann, and K. Kern, *Surf. Sci.* **389**, 366 (1997).
 - ⁴⁷M. B. Hugenschmidt, M. Ruff, A. Hitzke, and R. J. Behm, *Surf. Sci.* **388**, L1100 (1997).
 - ⁴⁸M. M. Dovek, C. A. Lang, J. Nogami, and C. F. Quate, *Phys. Rev. B* **40**, 11 973 (1989).
 - ⁴⁹C. A. Lang, M. M. Dovek, J. Nogami, and C. F. Quate, *Surf. Sci.* **224**, L947 (1989).
 - ⁵⁰R. A. Campbell, J. A. Rodriguez, and D. W. Goodman, *Phys. Rev.* **46**, 7077 (1992).
 - ⁵¹J. Wang, M. R. Vodd, H. Busse, and B. E. Koel, *J. Phys. Chem. B* **102**, 4693 (1998).
 - ⁵²M. Mavrikakis, P. Stoltze, and J. K. Nørskov, *Catal. Lett.* **64**, 101 (2000).
 - ⁵³E. Christoffersen, P. Liu, A. Ruban, H. L. Skriver, and J. K. Nørskov, *J. Catal.* **199**, 123 (2001).

- ⁵⁴P. Liu and J. K. Nørskov, *Phys. Chem. Chem. Phys.* **3**, 3814 (2001).
- ⁵⁵P. J. Schmitz, H. C. Kang, W. Y. Leung, and P. A. Thid, *Surf. Sci.* **248**, 287 (1991).
- ⁵⁶E. Christoffersen, P. Stoltze, and J. K. Nørskov, *Surf. Sci.* **505**, 200 (2002).
- ⁵⁷Private communication by A. S. Y. Chan and C. M. Friend.
- ⁵⁸A. Travert, H. Nakamura, R. A. van Santen, S. Cristol, J. F. Paul, and E. Payen, *J. Am. Chem. Soc.* **124**, 7084 (2002).
- ⁵⁹G. Wu, B. Bartlett, and W. T. Tysoe, *Surf. Sci.* **383**, 57 (1997).
- ⁶⁰M. Kamei, T. Obayashi, H. Tsunematsu, Y. Tanaka, and Y. Gotoh, *Surf. Sci.* **356**, 137 (1996).
- ⁶¹T. Sasaki, Y. Goto, R. Tero, K. Fukui, and Y. Iwasawa, *Surf. Sci.* **502**, 136 (2002).
- ⁶²H. Tøpsoe, B. S. Clausen, and F. E. Massoth, *Hydrotreating Catalysis* (Springer, New York, 1996).
- ⁶³J. C. Dunphy, C. Knight, P. Sautet, D. F. Ogletree, G. A. Somorjai, and M. B. Salmeron, *Surf. Sci.* **280**, 313 (1993).
- ⁶⁴S. Y. Li, J. A. Rodriguez, J. Hrbek, H. H. Huang, and G. Q. Xu, *Surf. Sci.* **366**, 29 (1996).
- ⁶⁵J. K. Nørskov, T. Bligaard, A. Logadottir, S. Bahn, L. B. Hansen, M. Bollinger, H. Benggaard, B. Hammer, Z. Sljivancanin, M. Mavrikakis, Y. Xu, S. Dahl, and C. J. H. Jacobsen, *J. Catal. Lett.* **209**, 275 (2002).
- ⁶⁶A. M. Molenbroek, J. K. Nørskov, and B. S. Clausen, *J. Phys. Chem. B* **105**, 5450 (2001).
- ⁶⁷P. L. Hansen, J. B. Wagner, S. Helveg, J. R. Rostrup-Nielsen, B. S. Clausen, and H. Topsøe, *Science (Washington, DC, U.S.)* **295**, 2053 (2002).